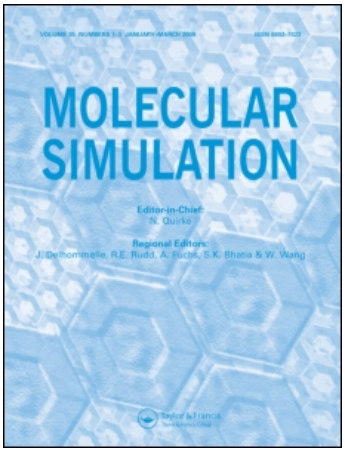

Molecular Simulation
Publication details, including instructions for authors and subscription information:
http://www.informaworld.com/smpp/title~content=t713644482

Conformational Correlations in DNA. Molecular Dynamics Studies

Witold R. Rudnicki[a]; Bogdan Lesyng[ab]
[a] Interdisciplinary Centre for Mathematical and Computational Modeling Warsaw University, Warsaw, Poland [b] Department of Biophysics, Warsaw University, Warsaw, Poland

To cite this Article Rudnicki, Witold R. and Lesyng, Bogdan(1997) 'Conformational Correlations in DNA. Molecular Dynamics Studies', Molecular Simulation, 19: 4, 247 — 266
To link to this Article: DOI: 10.1080/08927029708024154
URL: http://dx.doi.org/10.1080/08927029708024154

Molecular Simulation, 1997, Vol. 19, pp. 247–266
Reprints available directly from the publisher
Photocopying permitted by license only

CONFORMATIONAL CORRELATIONS IN DNA. MOLECULAR DYNAMICS STUDIES

WITOLD R. RUDNICKI[a] and BOGDAN LESYNG[a,b]

[a]*Interdisciplinary Centre for Mathematical and Computational Modeling Warsaw University, Banacha 2, 02-097, Warsaw, Poland;*
[b]*Department of Biophysics, Warsaw University, Żwirki i Wigury, 02-089, Warsaw, Poland*

(Received May 1996; Accepted December 1996)

A statistical, circular correlation model for conformational degrees of freedom in DNA is proposed. Correlation coefficients are computed for A and B DNA, as well as for transition processes between these forms, using microscopic MD simulation data. The correlations are interpreted and a minimal number of independent conformational degrees of freedom conserving basic static and dynamic properties of the right-handed DNA forms are found. The selected degrees of freedom form a hierarchical class and can constitute a base for a dynamical model using curvilinear degrees of freedom. In the most accurate representation one uses all backbone, torsional angles as well as pseudorotation parameters and glycosidic angles. In the second model one treats the backbone angles δ_i, and the glycosidic angles χ_i, as functions of the phases of pseudorotation, P_i. The third model assumes a functional dependence of other backbone angles ζ_i as functions of P_i.

Keywords: DNA; conformational transitions; molecular dynamics simulations; conformational correlations

1. INTRODUCTION

Conventional, microscopic molecular dynamics (MD) methods are used to simulate dynamical properties of biopolymers in a short time scale, usually in the range from 10^{-11} s to 10^{-9} s, see *e.g.* [1–3], while biologically interesting phenomena may occur in the time scale of 10^{-9} s to 10^{-3} s. This difference makes the direct MD simulations of most real phenomena difficult and special techniques have to be applied, see *e.g.* [4, 5] for selected methods of practical relevance. Inclusion of explicit water in the simulations

makes the problem even more difficult, since it increases the number of atoms in the system by five to twenty times. Increasing computer power is not sufficient to solve the problem and therefore development of new models and theories are of particular importance. There are several strategies of particular interest. The first one is a simplified description of solvent using various models [6–12]. Regardless of the method one tries to reduce the number of degrees of freedom in the system and increase the integration time-step, which typically is short, of the order of 10^{-15} s. An increase of the time-step can be achieved by introducing constraints, *e.g.*, by fixing bond lengths and/or bond angles, using for example the SHAKE algorithm [13, 14]. This increases the integration time step by a factor of 2 to 5. Another strategy uses a "reduced representation" or "succinct models", in which one surrenders the all-atom model by joining pieces of the structure into "united atoms" or "pseudoatoms", see *e.g.* [15–18]. An alternative method, which will be discussed in a greater detail, is based on internal, curvilinear degrees of freedom. This approach can lead both to a reduction in the number of degrees of freedom and an increase in the integration time step [19]. In the case of the DNA/RNA furanose ring we achieved a twenty-fold increase in the integration time step and fifty-fold reduction in the number of degrees of freedom. This approach can be applied to nucleic acids and in a further perspective to proteins.

In this work we try to answer the question how many independent degrees of freedom are required for the description of dynamical conformational changes in nucleic acids. Assuming that the bond lengths and bond angles are constant, we can describe the entire nucleic acid molecule using twelve torsional angles per residue: six angles along the backbone, five angles of the furanose ring and the glycoside bond angle. The pseudorotation model, [20–23] used for the description of the furanose ring, can further reduce the number of the degrees of freedom required for the description of nucleotide by expressing torsional angles in the ring as a function of two pseudorotation parameters, the phase and amplitude of pseudorotation. The amplitude of pseudorotation is fairly constant, thus we can describe the entire furanose ring with only one degree of freedom – the phase of pseudorotation. Therefore to describe the conformation of a single nucleotide we need eight degrees of freedom. It is well known, however, that there are still more correlations between the torsional angles in the nucleotides. In particular, the crystallographic studies, see *e.g.* [22, 24], suggest a strong correlation between torsional angles within a single nucleotide. These correlations could possibly be used for creating a reduced model of

nucleotides, with fewer independent degrees of freedom. Crystallographic correlations cannot be applied in MD studies directly, because the crystallographic data shows static correlations between average values of torsional angles. What is mostly required are instantaneous, dynamical correlations between conformational degrees of freedom. These correlations can be found using microscopic MD simulation data.

DNA is a flexible molecule and may adopt various structural conformations. All possible conformations are grouped into three families: A, B and Z DNA. B DNA is the standard, right-handed form, first postulated by Watson and Crick [25]. A DNA is a right-handed form as well, and Z DNA is a left-handed form. Z DNA is found in DNA fragments rich in G and C nucleic acid bases. *In vitro* the transition between A and B DNA is driven by changes in hydration processes, and the transition between B and Z mostly by changes in concentration of divalent cations. The important degree of freedom that influences the appearance of the helix is the furanose phase of pseudorotation [22].

In this study we present results of the MD simulations for a model DNA molecule in the A and B forms, as well as for intermediate states between them. The simulations results are analyzed and correlations between torsional angles are computed. The correlation analysis allows for selection of a minimal number of conformational degrees of freedom and this is the main purpose of this study. These degrees of freedom can further be used in the Lagrangian and Quaternion dynamics of DNA being developed in our laboratory.

2. METHODS

The molecular dynamics simulations were performed for 18 base pairs of a DNA fragment consisting of alternating G-C base pairs, in the A and B forms, and during the transition between these forms. Transitions between the A and B forms were simulated using two methods of enforcing desired conformational transformation, for details see paragraph 2.1. An extended circular correlation model was applied for calculating correlations between all conformationally important degrees of freedom, namely the torsional angles and pseudorotation parameters. In the third stage for each pair of conformational parameters (ϕ, θ) a nonlinear transformation $\phi \rightarrow \phi'$ was proposed in order to maximize a circular crosscorrelation coefficient $r_{\phi'\theta}$. This allowed to detect possible nonlinear correlations between the degrees of freedom.

2.1. Molecular Dynamics Simulations of Model DNA

An eighteen base pairs DNA fragment was built in standard A and B forms using the InsightII program [26]. The resulting structures were optimized by energy minimization in vacuo using the Amber [15] force field as implemented in the Discover 2.95 program [27], without explicit solvent, a distance dependent dielectric function $\varepsilon = r$ and with reduced phosphate charges, -0.3 for the A form, -0.7 for the B form, to account for solvent and ion effects. This parameterization was tested and compared with other commonly used force fields [28]. The energy minimization with this parameterization gave the closest overall similarity of the optimized structures with the PDB structural data.

The MD simulations were performed without explicit solvent, using the Discover 2.95 code of Biosym, with the same force field parameters. The following thermodynamic equilibration protocol was applied. The optimized structures were heated gradually to 300 K with a series of 0.1 ps MD simulations carried out in the microcanonical ensemble. The first simulation was carried out at 10 K and the temperature was increased by 10 K in each subsequent simulation. When the temperature reached 300 K, a 20 ps thermalization phase was carried out with coupling to a thermal bath using the Berendsen and Van Gunsteren method [29]. The velocity relaxation time τ was set to 0.1 ps. After thermalization a 200 ps production simulation was carried out with a weaker coupling to the thermal bath, $\tau = 1.0$ ps. The trajectories were stored every 50 fs for further analysis.

During the unconstrained MD simulation of A DNA, we observed a spontaneous transition of DNA from the A to B form. Our previous studies [28, 30] showed that in this force field, an effective potential for furanose has a global minimum in the S region. It occurs for conformations of the surrounding nucleotides typical for the B form of DNA. Therefore in simulations of the A form, local conformational fluctuations can trigger an irreversible transformation of the deoxyribose from the N to the S state, which results in the $A \rightarrow B$ transformation. Similar effects are also obtained by using an OPLS force field [31]. Also, modification of the electrostatic interactions, by replacing the atomic charges with the ESP charges calculated for the backbone atoms using a DFT method lead to similar results. We conclude that further improvements of the parametrization are required, but research in this direction was beyond the direct scope of this study. To prevent the spontaneous $A \rightarrow B$ transformation, we applied a procedure, based on a modification of the local pseudorotation potentials for each furanose ring, in a way similar to the umbrella sampling procedure,

see *e.g.* [1], which is routinely applied for sampling rarely accessed regions of the conformational space.

As mentioned, the conformational states of the furanose ring can be described by defining two parameters – the phase and amplitude of pseudorotation. Values of all torsional angles in the ring are then determined from the pseudorotation model. With the help of an additional harmonic torsional potential, we restrained the following two torsional angles, C1'-C2'-C3'-C4' and C2'-C3'-C4'-C5', of the furanose rings, see Figure 1, to the values predicted from the pseudorotation model for sugar in A DNA. In addition we used two methods to facilitate controlled transformations from A to B and from B to A. Both methods were based on modification of the local pseudorotation potentials, being simple extensions of the method used for stabilizing A DNA. In the first method we were changing the minimum of the auxiliary harmonic potential from 180° to 0° and back, to enforce $A \rightarrow B$ and $B \rightarrow A$ transformations, respectively. Hereafter this method is referred to as *synchronized* transformation. In the second

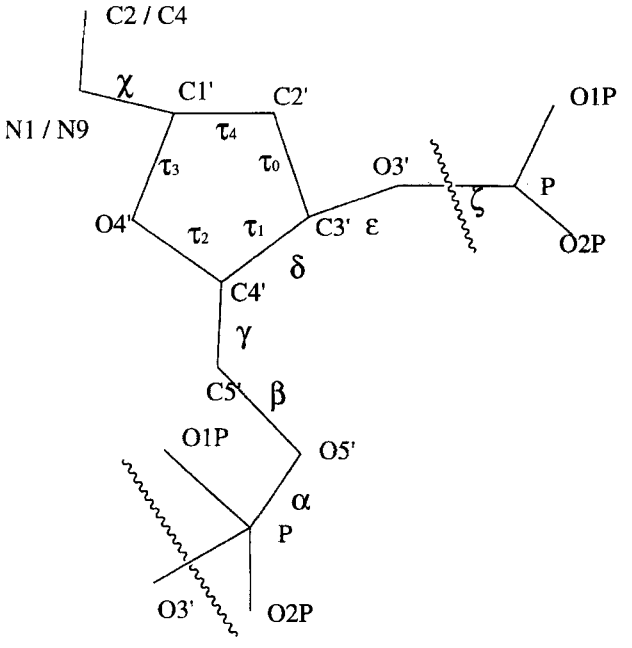

FIGURE 1 Nucleotide. Torsional angles are defined as follows: $\alpha = (O3', P, O5', C5')$, $\beta = (P, O5', C5', C4')$, $\gamma = (O5', C5', C4', C3')$, $\delta = (C5', C4', C3', O3')$, $\varepsilon = (C4', C3', O3', P)$, $\zeta = (C3', O3', P, O5')$, $\chi = (O4', C1', N1, C2_{purines}/C4_{pyrimidines})$, $\tau_0 = (C1', C2', C3', C4')$, $\tau_1 = (C2', C3', C4', O4')$, $\tau_2 = (C3', C4', O4', C1')$, $\tau_3 = (C4', O4', C1', C2')$, $\tau_4 = (O4', C1', C2', C3')$.

approach we localized the minimum of the auxiliary potential at 18°, corresponding to the canonical A form of DNA, and changed the strength of the auxiliary potential during the course of the simulation. To get the $A \rightarrow B$ transformation we started from an initial strong auxiliary potential and decrease it gradually to zero, and to get the $B \rightarrow A$ transformation we started from zero and gradually increased its strength. This procedure is called hereafter *nonsynchronized* transformation. In both types of simulations applied for the $A \rightarrow B$ and $B \rightarrow A$ transformations we used the same thermalization procedure as described above. In the synchronized transformation the production phase consisted of 180 ps dynamics with the minimum of the auxiliary potential moving with the rate of 1°/ps. The force constant of the restrained torsional potential was set to 20 kcalmol^{-1} rad^{-2}. The synchronized transformation of the furanose rings results in a reaction of other degrees of freedom – the correlation we are interested in. In the nonsynchronized transformation production phase consisted of 200 ps dynamics and the initial force constant of the forcing potential was set to 2 kcalmol^{-1} rad^{-2} (0 kcalmol^{-1} rad^{-2}) and decreased (increased) by 0.5 kcalmol^{-1} rad^{-2} every 5 ps for the $A \rightarrow B (B \rightarrow A)$ transformation.

2.2. Circular Correlation Model

It is well known, that a standard statistical analysis is not well suited for the description of periodic, torsional variables. Take for example the average of the two angles 10° and 350°. We can get a reasonable value of the average by transforming the domain from [0°, 360°] to [−180°, 180°], but the problem will just reappear for angles close to 180°. To solve the problem Kitamura and co-workers have introduced a circular correlation method [24]. Here we present a similar method, for calculating basic statistical properties of the periodic variables. Our method is a formal extension of the ordinary statistical analysis applied to the domain of angular variables.

We will start by extending the ordinary statistical analysis into an N-dimensional vector space. First, let us recollect the definitions of the basic statistical quantities and write them in a vector notation. We will use lower case letters to denote statistical variables and capital letters to denote average values of statistical variables, in particular:
mean

$$\vec{U} = \frac{\sum_{i=1}^{N} \vec{u}_i}{N}, \tag{1}$$

variance

$$VAR_u = \frac{\Sigma_{i=1}^{N}(\vec{u}_i - \vec{U})(\vec{u}_i - \vec{U})}{N} = \frac{\Sigma_{i=1}^{N}(\vec{u}_i\vec{u}_i - \vec{U}\vec{U})}{N}, \tag{2}$$

standard deviation

$$\sigma_u = \sqrt{VAR_u}, \tag{3}$$

covariance of two variables $\vec{u}_i$ and $\vec{w}_i$

$$COV_{uw} = \frac{\Sigma_{i=1}^{N}(\vec{u}_i - \vec{U})(\vec{w}_i - \vec{W})}{N} = \frac{\Sigma_{i=1}^{N}(\vec{u}_i\vec{w}_i - \vec{U}\vec{W})}{N}, \tag{4}$$

and a linear correlation coefficient

$$r_{uw} = \frac{COV_{uw}}{\sigma_u\sigma_w}. \tag{5}$$

Note that we can represent the angular variable ϕ as a two dimensional vector of a unit length, $\vec{u} = (\cos(\phi), \sin(\phi))$.

We may find the average of the set of phase angles $\{\phi_i\}$ by calculating the average vector $\vec{U}$ from the set $\{\vec{u}_i\}$. Let Φ denote the phase angle of the $\vec{U}$ vector.

$$\vec{U} = \frac{\Sigma_i^N \vec{u}_i}{N} = \frac{\Sigma_i^N(\cos(\phi), \sin(\phi))}{N}, \tag{6}$$

and

$$\vec{U} = (|U|\cos\Phi, |U|\sin\Phi). \tag{7}$$

$|U|$ is the length of the average vector, which gives us information about variance of the variable u. For a set of closely packed u_i we expect U to be close to 1, while for random uncorrelated data U should be close to zero. This obvious statement can be derived in a more formal way – based on our derivation of variance,

$$VAR_u = \frac{\Sigma_{i=1}^{N}(\vec{u}_i\vec{u}_i - \vec{U}\vec{U})}{N} = \frac{\Sigma_{i=1}^{N}(1 - \vec{U}\vec{U})}{N}, = 1 - |U|^2. \tag{8}$$

In a similar way we can derive the circular correlation coefficient for the angular variables ϕ and θ. Let u and w be their respective vector variables. The covariance of ϕ and θ can be obtained from Eq. 4 as

$$COV_{\phi\theta} = \frac{\Sigma_i^N [\cos(\phi_i - \theta_i) - |U||W| \cos(\Phi - \Theta)]}{N}. \tag{9}$$

The correlation coefficient can be found from the relation (5),

$$r_{\phi\theta} = \frac{COV_{\phi\theta}}{\sigma_\phi \sigma_\theta} = \frac{\Sigma_i^N [\cos(\phi_i - \theta_i) - |U||W| \cos(\Phi - \Theta)]}{\sqrt{1 - |U|^2}\sqrt{1 - |W|^2}}, \tag{10}$$

2.3. Searching for Interdependent Conformational Parameters

The goal of our work is to reduce the number of degrees of freedom required for the description of conformation of nucleic acids. We computed the circular correlation coefficients for all pairs of conformational degrees of freedom to find possible relations between them. For selected pairs we took an additional step and checked possible nonlinear correlations. The linear correlation coefficient is a measure of a linear dependence between statistical variables, but it may not be sufficient for a more complicated interdependence – an obvious example is the case when the points in the configuration space are located on the circle. To detect possible simple nonlinear correlations we used a simple transformation of a variable ϕ in the form

$$\phi' = a\phi + b + c \sin(\phi) + d \cos(\phi), \tag{11}$$

and computed the correlation coefficients (Eq. 10) of the transformed variable ϕ' with other variables. We tested nonlinear correlations for selected pairs of conformational degrees of freedom by calculating first $r_{\phi'\theta}$ and then $r_{\phi\theta'}$. The parameters for the nonlinear model were obtained by minimizing the root mean square deviation between the transformed, ϕ'_i, and simulation data, θ_i,:

$$\text{RMS} = \sqrt{\frac{\Sigma_i^N (\phi'_i - \theta_i)^2}{N}}. \tag{12}$$

The data was collected separately for each residue of the 16 base pairs in the inner part of the molecule, and after that averaged to obtain a single data

set for the whole molecule. We computed correlations of the torsional parameters of the i-th residue with the parameters from the residues $i-1$, i and $i+1$. The analysis of the correlations between various degrees of freedom was carried out separately for the A and B forms and for all simulated transitions between these forms. The results of various simulations were compared.

3. RESULTS AND DISCUSSION

3.1. Dynamics

During the simulations of A DNA, with the stabilising procedure described earlier, the deoxyribose rings stayed in the N region of the pseudorotational circle. The evolution of the pseudorotation phase from 28 central deoxyribose rings in the constrained simulation are shown in Figure 2a. The evolution of the backbone torsional angles, pseudorotation phase and the glycosidic angle χ, during the constrained simulation, from a selected single residue are shown in Figure 3a.

During the simulations of B DNA its structure was stable, with small oscillations around the average conformation. The sugar rings stayed in the S region of the pseudorotation circle, with rare, rapid repuckering to the N region, in 1ps time intervals. The evolution of the pseudorotation phase for 28 central deoxyribose rings is shown in Figure 2b. The evolution of the backbone torsional angles, pseudorotation phase P and the glycosidic angle χ for a selected single residue is shown in Figure 3b. The correlations between P, χ and δ are easily visible.

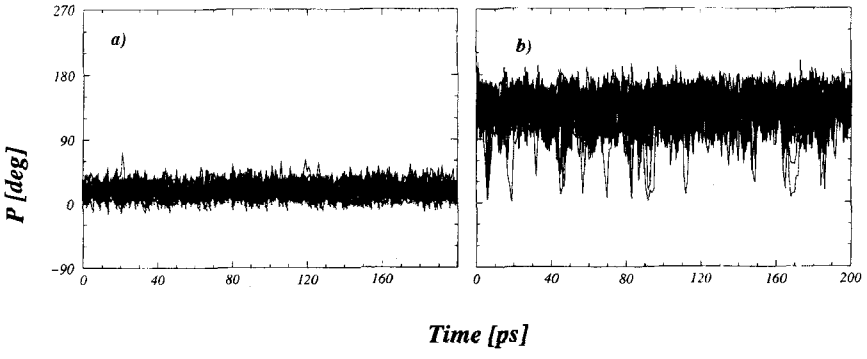

FIGURE 2 Pseudorotation phase of 28 deoxyribose rings during simulation of the A DNA, a), and B DNA, b), fragments.

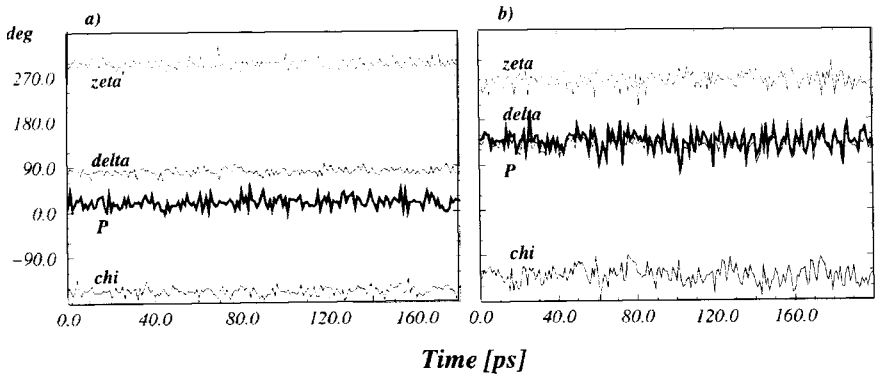

FIGURE 3 Selected backbone torsional angles, pseudorotation phase P and χ of a selected single residue, during the simulation of the A DNA, a), and B DNA, b), fragment.

Both methods of enforcing the DNA transitions were successful, and we obtained the $A \rightarrow B$ and $B \rightarrow A$ transitions using the synchronized and nonsynchronized procedures for sugar conformational transitions. As should be expected during the synchronized transition the pseudorotation phases of rings were strongly correlated and constrained to a narrow range around the mean value. During the nonsynchronized transition the variation of the pseudorotation phases was much larger (see Fig. 4). In the synchronized transformation the $A \rightarrow B$ and $B \rightarrow A$ transitions are achieved by a synchronized change of the pseudorotation phase off all sugar rings. On the other hand, in the nonsynchronized transformation the $A \rightarrow B$ and $B \rightarrow A$ transitions are achieved by an increased frequency of switching the deoxyribose conformation from the initial to the final domain of the pseudorotational circle, and by increasing the life time in the final conformation.

This difference is also evident in the evolution of the conformational parameters of a single nucleotide. During the synchronized transition we observe a gradual change of the pseudorotation phases P and changes of the correlated angles δ and χ. On the other hand, during the nonsynchronized transitions, we observe single-step transformation between S and N conformations of deoxyribose (see Fig. 5).

3.2. Correlations between Conformational Parameters

As mentioned the goal of this study is to identify the correlations that potentially can be used for building the simplified model of DNA, with a reduced total number of degrees of freedom required for the description of DNA dynamics. In the ideal case, a strong correlation between two degrees

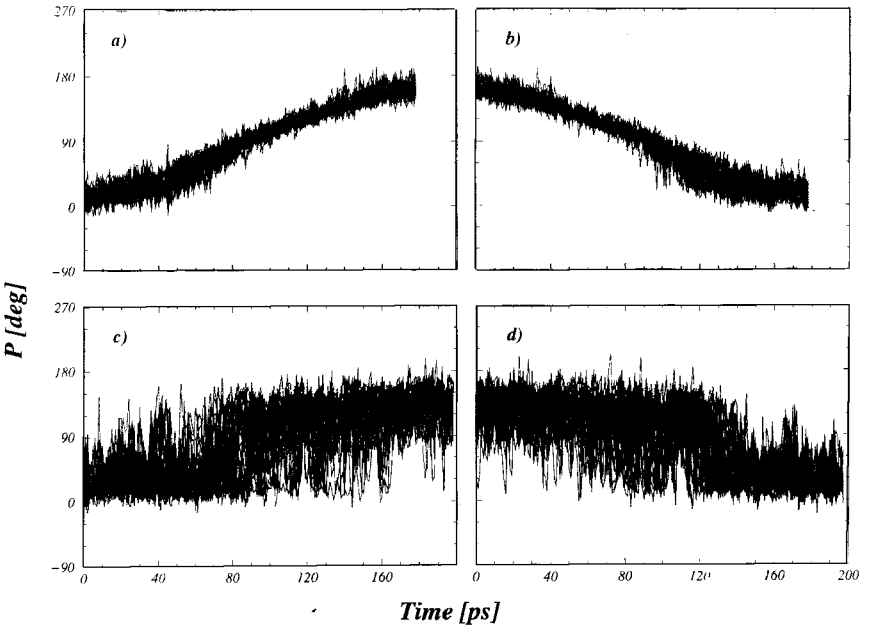

FIGURE 4 Pseudorotation phase of 28 central deoxyribose rings, during the synchronized $A \rightarrow B$, a), $B \rightarrow A$, b), and nonsynchronized $A \rightarrow B$, c), $B \rightarrow A$, d), transformations of DNA.

of freedom allows us to reduce motion on the two-dimensional hypersurface to a motion along a one-dimensional curve on this hypersurface.

We observed three different types of relations between the torsional angles in various MD simulations the correlations within the furanose ring which are described by the pseudorotation model and will not be discussed here. In A DNA we have not observed any significant correlations between the torsional angles. In B DNA two torsional angles, e. e. δ, and χ, were correlated with the phase of pseudorotation P. During the simulated transitions between the A and B forms three torsional angles, e. e. δ, ζ and χ, were correlated with the phase of pseudoration P. We have not discovered any significant correlations between torsional angles of adjacent nucleotides, see Table I. Therefore in further discussion we will concentrate on the correlations within a single nucleotide.

3.2.1. Correlations in the A and B Forms of DNA

We have not discovered any significant correlations between the torsional angles in A DNA (Tab. II). In contrast, we observed significant correlation

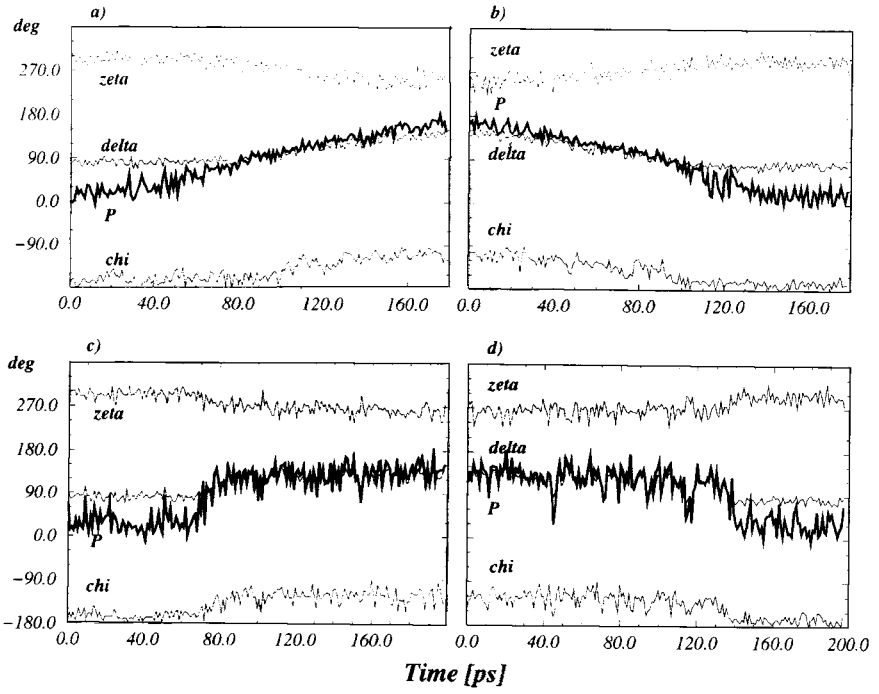

FIGURE 5 Selected torsional parameters during the synchronized $A \rightarrow B$, a), $B \rightarrow A$, b), and nonsynchronized $A \rightarrow B$, c), $B \rightarrow A$, d), transformations of DNA.

TABLE I Absolute values of the circular correlation coefficients between all conformational parameters of the adjoining nucleotides i and $i-1$ in B-DNA. Values smaller than 0.15 neglected

	α	β	γ	δ	ε	ζ	χ	τ_0	τ_1	τ_2	τ_3	τ_4	τ_m	P
α	–	0.17	–	–	–	–	–	–	0.16	–	–	–	–	–
β	–	–	–	–	0.34	–	–	–	–	–	–	–	–	–
γ	–	0.20	–	–	–	–	–	–	–	–	–	–	–	–
δ	–	–	–	–	–	–	–	–	–	–	–	–	–	–
ε	0.17	–	–	–	–	0.19	–	–	–	–	–	–	–	–
ζ	0.16	–	–	–	–	–	–	–	–	–	–	–	–	–
χ	–	–	–	–	–	–	–	–	–	–	–	–	–	–
τ_0	–	–	–	–	–	–	–	–	–	–	–	–	–	–
τ_1	–	–	–	–	–	0.16	–	–	–	–	–	–	–	–
τ_2	–	–	–	–	–	0.19	–	–	–	–	–	–	–	–
τ_3	–	–	–	–	–	–	–	–	–	–	–	–	–	–
τ_4	–	–	–	–	–	–	–	–	–	–	–	–	–	–
τ_m	–	–	–	–	–	–	–	–	–	–	–	–	–	–
P	–	–	–	–	–	–	–	–	–	–	–	–	–	–

TABLE II Absolute values of the circular correlation coefficients between all conformational parameters in the nucleotides in A-DNA. Values smaller than 0.35 neglected

	α	β	γ	δ	ε	ζ	χ	τ_0	τ_1	τ_2	τ_3	τ_4	τ_m	P
α	1	–	–	–	–	–	–	–	–	–	–	–	–	–
β	–	1	–	–	–	–	–	–	–	–	–	–	–	–
γ	–	–	1	–	–	–	–	–	–	–	–	–	–	–
δ	–	–	–	1	–	–	–	–	–	–	–	–	–	–
ε	–	–	–	–	1	–	–	–	–	–	–	–	–	–
ζ	–	–	–	–	–	1	–	–	–	–	–	–	–	–
χ	–	–	–	–	–	–	1	–	–	–	–	–	–	–
τ_0	–	–	–	–	–	–	–	1	0.42	–	0.49	0.85	–	0.68
τ_1	–	–	–	–	–	–	–	0.42	1	–	–	0.45	0.78	0.55
τ_2	–	–	–	–	–	–	–	–	–	1	–	0.35	–	–
τ_3	–	–	–	–	–	–	–	0.49	–	–	1	0.82	–	0.92
τ_4	–	–	–	–	–	–	–	0.85	0.45	0.35	0.82	1	–	0.90
τ_m	–	–	–	–	–	–	–	–	0.78	–	–	–	1	–
P	–	–	–	–	–	–	–	0.68	0.55	–	0.92	0.90	–	1

TABLE III Absolute values of the circular correlation coefficients between all conformational parameters in the nucleotides in B-DNA. Values smallar than 0.35 neglected

	α	β	γ	δ	ε	ζ	χ	τ_0	τ_1	τ_2	τ_3	τ_4	τ_m	P
α	1	–	–	–	–	–	–	–	–	–	–	–	–	–
β	–	1	–	–	–	–	–	–	–	–	–	–	–	–
γ	–	–	1	–	–	–	–	–	–	–	–	–	–	–
δ	–	–	–	1	–	0.35	–	–	0.54	0.42	–	0.35	–	0.87
ε	–	–	–	–	1	–	–	–	–	–	–	–	–	–
ζ	–	–	–	0.35	–	1	–	–	–	–	–	–	–	–
χ	–	–	–	–	–	–	1	–	–	0.37	0.46	–	–	–
τ_0	–	–	–	–	–	–	–	1	0.62	0.49	–	–	0.57	–
τ_1	–	–	–	0.54	–	–	–	0.62	1	0.85	0.54	–	–	0.51
τ_2	–	–	–	0.42	–	–	0.37	0.49	0.85	1	0.84	–	–	0.51
τ_3	–	–	–	–	–	–	0.46	–	0.54	0.84	1	0.47	–	–
τ_4	–	–	–	0.35	–	–	–	–	–	–	0.47	1	–	0.50
τ_m	–	–	–	–	–	–	–	0.57	–	–	–	–	1	–
P	–	–	–	0.87	–	–	–	–	0.51	0.51	–	0.50	–	1

of δ with the pseudorotation phase P in B DNA, (Tab. III). This difference can be explained by a different scale of fluctuations of δ and P in A and B DNA. In A DNA only relatively small fluctuations from the average values are allowed, while in B DNA the fluctuations are much larger, see Figure 6. It's worth noting that the configuration space allowed energetically for A DNA in our simulations is a subset of the space allowed for B DNA.

In B DNA the correlation coefficients between δ and nonlinearly transformed P, as well as between χ and nonlinearly transformed P were significantly higher than respective correlation coefficients between δ, χ and P, (Tab. V). The increase of the correlations was even more evident for angles

inside the furanose ring, both for the A and B forms, see Tables IV and V. This confirms successful application of the nonlinear transformation for detecting the correlations.

3.2.2. *Correlations during Transitions between the A and B Forms of DNA*

In all transitions between the A and B forms of DNA, the observed correlations between P and the backbone torsional angles are very similar, independent of the method of enforcing the transformations and their direction.

TABLE IV Absolute values of the circular correlation coefficients between nonlinearly transformed conformational parameters (column) and conformational parameters (row) for the nucleotides in A-DNA. Values smallar than 0.5 neglected

	α	β	γ	δ	ε	ζ	χ	τ_0	τ_1	τ_2	τ_3	τ_4	τ_m	P
α	1	–	–	–	–	–	–	–	–	–	–	–	–	–
β	–	1	–	–	–	–	–	–	–	–	–	–	–	–
γ	–	–	1	–	–	–	–	–	–	–	–	–	–	–
δ	–	–	–	1	–	–	–	–	–	–	–	–	–	–
ε	–	–	–	–	1	–	–	–	–	–	–	–	–	–
ζ	–	–	–	–	–	1	–	–	–	–	–	–	–	–
χ	–	–	–	–	–	–	1	–	–	–	–	–	–	–
τ_0	–	–	–	–	–	–	–	1	0.80	–	0.74	0.93	–	0.93
τ_1	–	–	–	–	–	–	–	0.80	1	–	–	0.56	0.78	0.56
τ_2	–	–	–	–	–	–	–	–	–	1	0.72	–	0.83	–
τ_3	–	–	–	–	–	–	–	0.74	–	0.71	1	0.92	–	0.92
τ_4	–	–	–	–	–	–	–	0.93	0.56	–	0.93	1	–	0.99
τ_m	–	–	–	–	–	–	–	–	0.77	0.83	–	–	1	–
P	–	–	–	–	–	–	–	0.93	0.60	–	0.93	0.99	–	1

TABLE V Absolute values of the circular correlation coefficients between nonlinearly transformed conformational parameters (column) and conformational parameters (row) for the nucleotides in B-DNA. Values smallar than 0.5 neglected

	α	β	γ	δ	ε	ζ	χ	τ_0	τ_1	τ_2	τ_3	τ_4	τ_m	P
α	1	–	–	–	–	–	–	–	–	–	–	–	–	–
β	–	1	–	–	–	–	–	–	–	–	–	–	–	–
γ	–	–	1	–	–	–	–	–	–	–	–	–	–	–
δ	–	–	–	1	–	–	0.57	0.70	0.89	0.91	0.83	0.52	–	0.88
ε	–	–	–	–	1	–	–	–	–	–	–	–	–	–
ζ	–	–	–	–	–	1	–	–	–	–	–	–	–	–
χ	–	–	–	0.58	–	–	1	–	0.57	0.61	0.57	–	–	0.58
τ_0	–	–	–	0.55	–	–	–	1	0.83	0.58	–	–	0.77	0.63
τ_1	–	–	–	0.87	–	–	0.55	0.87	1	0.94	0.76	–	–	0.91
τ_2	–	–	–	0.91	–	–	0.60	0.75	0.95	1	0.94	0.66	–	0.97
τ_3	–	–	–	0.84	–	–	0.57	–	0.75	0.92	1	0.77	–	0.88
τ_4	–	–	–	–	–	–	–	0.51	–	–	0.75	1	0.74	0.50
τ_m	–	–	–	–	–	–	–	0.57	–	–	–	0.69	1	–
P	–	–	–	0.91	–	–	0.57	0.84	0.91	0.98	0.94	0.83	–	1

The correlations between δ, χ and P are similar to the correlations observed in the simulations for B DNA. The projections of the phase-space trajectory onto the coordinate subspace (P, δ) and (P, χ) for all simulated transitions are very similar to the analogous projections from the B DNA simulation, see Figure 7 and Figure 8. In all simulated transitions the new correlation

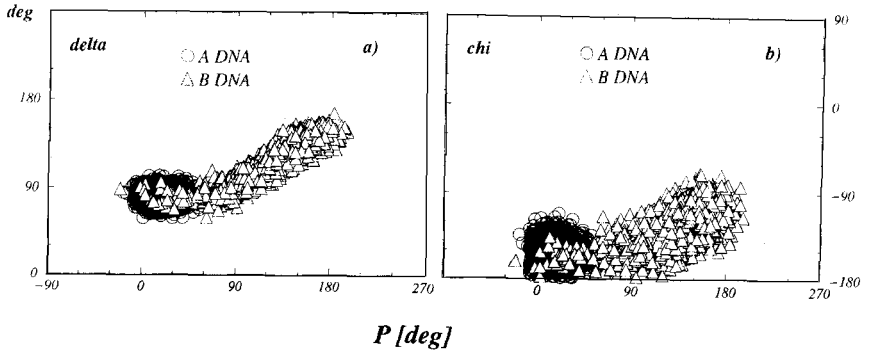

FIGURE 6 Projection of the phase-space trajectories onto the (P, δ), a), and (P, χ), b), subspaces, for the A and B forms of DNA.

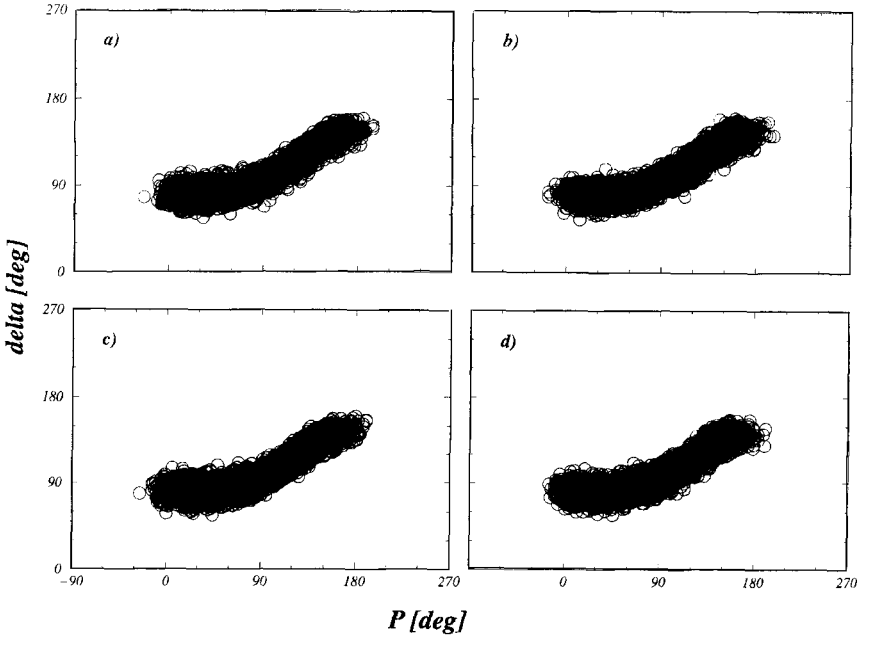

FIGURE 7 Projection of the phase-space trajectories onto the (P, δ) subspace for the synchronized $A \rightarrow B$, a), $B \rightarrow A$, b), and nonsynchronized $A \rightarrow B$, c), $B \rightarrow A$, d), transformations of DNA.

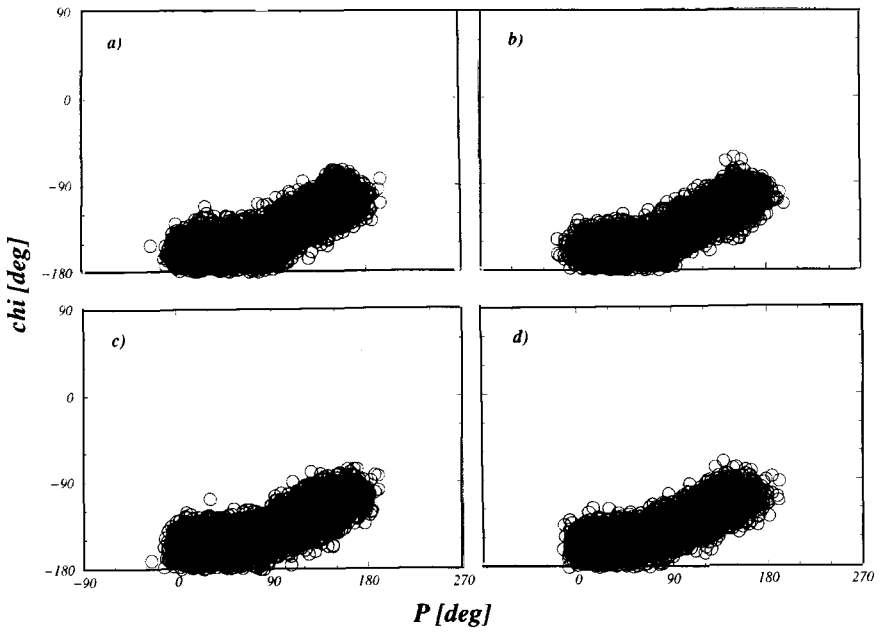

FIGURE 8 Projection of the phase-space trajectories onto the (P, χ) subspace for the synchronized $A \rightarrow B$, a), $B \rightarrow A$, b), and nonsynchronized $A \rightarrow B$, c), $B \rightarrow A$, d), transformations of DNA.

between P and ζ is found. The nonlinear transformation of the pseudorotation phase P increases the correlation coefficient for all torsional angles δ, χ and ζ, see Tables VI and VII.

3.2.3. *Convergence of the Correlations*

Convergence of the correlations for the most important degrees of freedom is presented in Figure 9. The circular correlations obtained in the simulations of the A and B forms converge to their equilibrium values during less than 10 picoseconds, see Figure 9a. During the transitions between the A and B forms correlations computed in consecutive 10 ps periods are variable, they converge, however, to the local equilibrium values represented by the correlations measured in the 20 ps intervals, see Figure 9b. The correlations are relatively high in the part of the trajectory for which DNA adopts the B DNA form, albeit lower than for the unconstrained simulation, and very low in the part of the trajectory for which DNA adopts the A DNA form. That suggests, that the forcing potential imposed on the furanose ring has only a limited influence on the correlations.

TABLE VI Absolute values of the circular correlation coefficients of selected torsional angles and P during the two enforced transformations between the A and B forms of DNA

Method	*Transition*	α	β	γ	δ	ε	ζ	χ
Synchronized	$A \rightarrow B$	0.25	0.06	0.24	0.84	0.07	0.67	0.53
	$B \rightarrow A$	0.25	0.09	0.25	0.86	0.12	0.69	0.56
Nonsynchronized	$A \rightarrow B$	0.26	0.07	0.18	0.84	0.20	0.66	0.58
	$B \rightarrow A$	0.16	0.06	0.19	0.84	0.14	0.58	0.60

TABLE VII Absolute values of the circular correlation coefficients of selected torsional angles with the nonlinearly transformed pseudorotation phase P during the two enforced transformation between the A and B forms of DNA

Method	*Transition*	α	β	γ	δ	ε	ζ	χ
Synchronized								
	$A \rightarrow B$	0.30	0.26	0.32	0.96	0.41	0.74	0.85
	$B \rightarrow A$	0.29	0.30	0.33	0.96	0.42	0.75	0.86
Nonsynchronized								
	$A \rightarrow B$	0.31	0.29	0.21	0.95	0.41	0.75	0.82
	$B \rightarrow A$	0.22	0.26	0.22	0.94	0.34	0.64	0.84

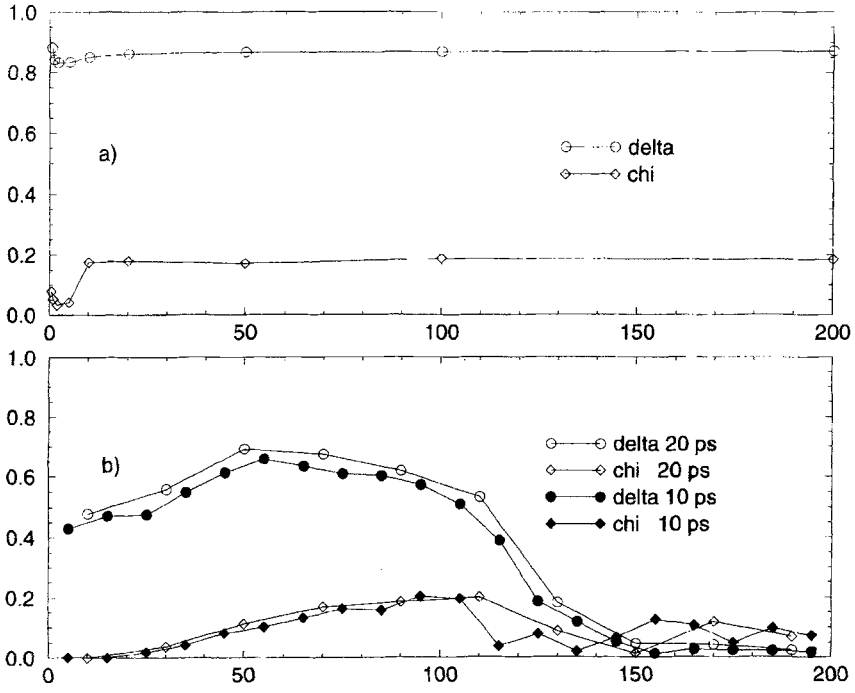

FIGURE 9 Covergence of the simulations a) circular correlation coefficients for the δ and χ torsion angles as functions of the simulation time for B DNA, b) circular correlation coefficients computed for 10 and 20 ps intervals during the synchronized $B \rightarrow A$ transformation of DNA.

4. CONCLUSIONS

The main goal of this study was finding correlations between the conformational parameters that can be used for the construction of the reduced dynamical model of nucleic acids. The results are the following:

Circular correlations between the conformational parameters differ in the A and B DNA forms and during transitions between them. B DNA is the flexible form, for which some parameters, like phase of pseudorotation P and torsional angles δ and χ, change to a significant degree. On the other hand A DNA, within the restraints imposed on the deoxribose ring, to preserve it's 3'-endo conformation, is more rigid, where only small deviations from the mean values are allowed. The conformational region occupied by the phase-space trajectories of A DNA, projected onto the (P, δ) and (P, χ) subspaces, is a subset of the B DNA one.

The circular correlation analysis shows the existence of two subsets of the torsional parameters. The first one is the set correlated to the pseudorotation phase, consisting of the ring torsion angles τ_i, δ and χ, as well as ζ in the case of the transitions between the A and B forms. The second set consists of the other backbone torsional angles. They are correlated neither with the ring angles, nor with other backbone angles.

The correlations between P and δ, and between P and χ observed during the simulated transitions between the A and B forms are similar to the correlations observed for the B form.

The convergence analysis shows, that our restraining potential has only a limited influence on the correlations observed in B DNA. Introducing the potential doesn't change any qualitative conclusions. We believe it is also true for A DNA.

The results suggest three possible models of DNA. In the most accurate model one should use all backbone torsional angles, pseudorotation parameters P and τ_m, as well as the glycosidic angle χ. In the second model one can replace δ and χ by the functions of the pseudorotation phase P. This model should accurately reproduce dynamics of B DNA and transitions between the two forms, but would probably introduce strong constraints on A DNA. In the third, least accurate model, one may replace δ, ζ and χ by the functions of the pseudorotation phase P. This model may be suitable for mean field simulations of DNA, where short time scale effects can be neglected.

Our study shows that the correlations between fluctuations of the torsional angles around their average values, within a single nucleotide, are not as strong as the correlations between average values found in various structures observed crystallographically.

Acknowledgements

The studies were supported by the State Committee for Scientific Research within the project 2 P302 029 07. Funds for the update of the MSI software were provided within the project 8 T11F 006 09. The simulations were performed in the Interdisciplinary Centre for Mathematical and Computational Modelling at the Warsaw University.

References

[1] McCammon, J. A. and Harvey, S. C. (1987). *Dynamics of Proteins and Nucleic Acids*, (Cambridge University Press, London).
[2] van Gunsteren, W. F., Weiner, P. K. and Wilkinson, A. J., (Eds.), (1993). *Computer Simulations of Biomolecular Systems*, (ESCOM, Leiden).
[3] Lesyng, B. and McCammon, J. A. (1993). "Molecular modeling methods. Basic techniques and challenging problems", *Pharmac. Ther*, **60**, 149.
[4] Straatsma, T. and McCammon, J. A. (1992). "Computational alchemy", *Ann. Rev. of Phys. Chem.*, **43**, 407.
[5] Elber, R. and Karplus, M. (1990). "Enhanced sampling in molecular dynamics: Use of the time dependent Hartree approximation for a simulation of carbon monoxide through myoglobin", *J. Amer. Chem. Soc.*, **112**, 9161.
[6] Smith, P. E. and Pettitt, B. M. (1994). "Modeling solvent in biomolecular systems", *J. Phys. Chem.*, **98**, 9700.
[7] Greengard, L. and Rokhlin, V. J. (1987). "A fast algorithm for particle simulations", *J. Comput. Phys.*, **73**, 325.
[8] Ding, H., Karasawa, N. and Goddard, W. A. III (1994). "Modeling solvent in biomolecular systems", *J. Chem. Phys.*, **97**, 4309.
[9] Smith, P. E. and van Gunsteren, W. F. (1993). "Methods for the evaluation of long range electrostatic forces in computer simulations of molecular systems", in: van Gunsteren, W. F., Weiner, P. K. and Wilkinson, A. J., (Eds.) *Computer Simulations of Biomolecular Systems: Theoretical and Experimental Applications*, (Leiden), 182.
[10] van Gunsteren, W. F. and Berendsen, H. J. C. (1990). "Computer simulations of molecular dynamics – methodology, applications, and perspectives in chemistry", *Angew. Chem., Int. Ed. Engl.*, **29**, 992.
[11] Allen, M. P. and Tildesley, D. J. (1987). *Computer simulations of liquids*, (Clarendon Press, Oxford, 1987).
[12] Rudnicki, W. R. and Pettitt, B. M. (in press). "Modeling of the DNA-water interface", *Biopolymers*.
[13] van Gunsteren, W. F. (1980). "Constrained dynamics of flexible molecules", *Mol. Phys.*, **40**, 1015.
[14] Ryackert, J. P., Ciccotti, G. and Berendsen, H. J. C. (1977). "Numerical integration of the cartesian equations of motion of a system with constraints: molecular dynamics of n-alkanes", *J. Comp. Phys.*, **23**, 327.
[15] Weiner, S. J., Kollman, P. A., Case, D. A., Singh, U. S., Ghio, C., Alagona, G., Profeta, S., Jr. and Weiner, P. (1984). "A new force field for molecular mechanical simulation of nucleic acids and proteins", *J. Am. Chem. Soc.*, **106**, 755.
[16] van Gunsteren, W. F., Berendsen, J. H. C., Hermans, J., Hol, W. G. and Postma, J. P. M. (1983). "Computer simulation of the dynamics of hydrated protein crystals and its comparison with X-ray data", *Proc. Natl. Acad. Sci. USA*, **80**, 4315.
[17] Brooks, B. R., Bruccoleri, R. E., Olafson, B. D., States, D. J., Swaminathan, S. and Karplus, M. (1983). "CHARMM: A program for macromolecular energy, minimization and dynamics calculations", *J. Comput. Chem.*, **4**, 187.

[18] Tan, R. K.-Z., Sprous, D. and Harvey, S. C. (1996). "Molecular dynamics simulations of small DNA plasmids: Effects of sequence and supercoiling on intramolecular motions", *Biopolymers*, **39**(2), 259.
[19] Rudnicki, W. R., Lesyng, B. and Harvey, S. C. (1994). "Lagrangian molecular dynamics using selected conformational degrees of freedom, with application to the pseudorotation dynamics of furanose rings", *Biopolymers*, **34**, 383.
[20] Cremer, D. and Pople, J. A. (1975). "A general definition of ring puckering coordinates", *J. Am. Chem. Soc.*, **97**, 1354.
[21] Altona, C. and Sundaralingam, M. (1972). "Conformational analysis of the sugar ring in nucleosides and nucleotides. A new description using the concept of pseudorotation", *J. Am. Chem. Soc.*, **94**, 8205.
[22] Saenger, W. (1983). *Principles of Nucleic Acids Structure*, (Springer-Verlag, New York).
[23] Lesyng, B. (1987). "Barrier to pseudorotation of furanose rings and its biological implications", in: *Topics in Nucleic Acids Strture. Part 3.*, Neidle, S., (Ed.), (Macmillan, London), p. 71.
[24] Kitamura, K., Wakahara, A., Mizuno, H., Baba, Y. and Tomita, K. (1981). "Conformationally "concerted" changes in nucleotide structures. A new description using circular correlation and regression analysis", *J. Am. Chem. Soc.*, **103**, 3899.
[25] Watson, J. D. and Crick, F. H. C. (1953). "A structure for a deoxyrybonucleic acid", *Nature*, **171**, 737.
[26] *Insight User Guide, Version 2.35*, (Biosym Technologies, San Diego) (1994).
[27] *Discover User Guide, Version 2.95*, (Biosym Technologies, San Diego) (1994).
[28] Rudnicki, W. R. and Lesyng, B. (1995). "Applicability of commonly used atom-atom type potential energy functions in structural analysis of nucleic acids. The role of electrostatic interactions", *Comp. and Chem.*, **19**(3), 253.
[29] Berendsen, H. J. C., Postma, J. P. M., van Gunsteren, W. F., DiNola, A. and Haak, J. R. (1984). "Molecular dynamics with coupling to an external bath", *J. Chem. Phys.*, **8**, 3684.
[30] Pechenaya, V., Rudnicki, W. R., Grycuk, T. and Lesyng, B. (1995). "Pseudorotation potential of deoxyribose in double-helical C, G oligonucleotides", *Molecular Biology, Rus. ed.*, **29**(5), 616.
[31] Jorgensen, W. L. and Tirado-Rives, J. (1988). "The OPLS potential functions for proteins. Energy minimizations for crystals of cyclic peptides and crambin", *J. Am. Chem. Soc.*, **110**, 1657.